Quantum Phase Diagram of Bosons in Optical Lattices

Ednilson Santos, Matthias Ohliger, Alexander Hoffmann, and Axel Pelster

LMU ARNOLD SOMMERFELD CENTER FOR THEORETICAL PHYSICS

UNIVERSITÄT DUISBURG ESSEN

Outline of the talk

1. Experimental facts
2. Theoretical description
3. Mean-field theory
4. State of the art
5. Effective potential method
6. Green's function method
7. Results
8. Conclusion

1 - Experimental facts

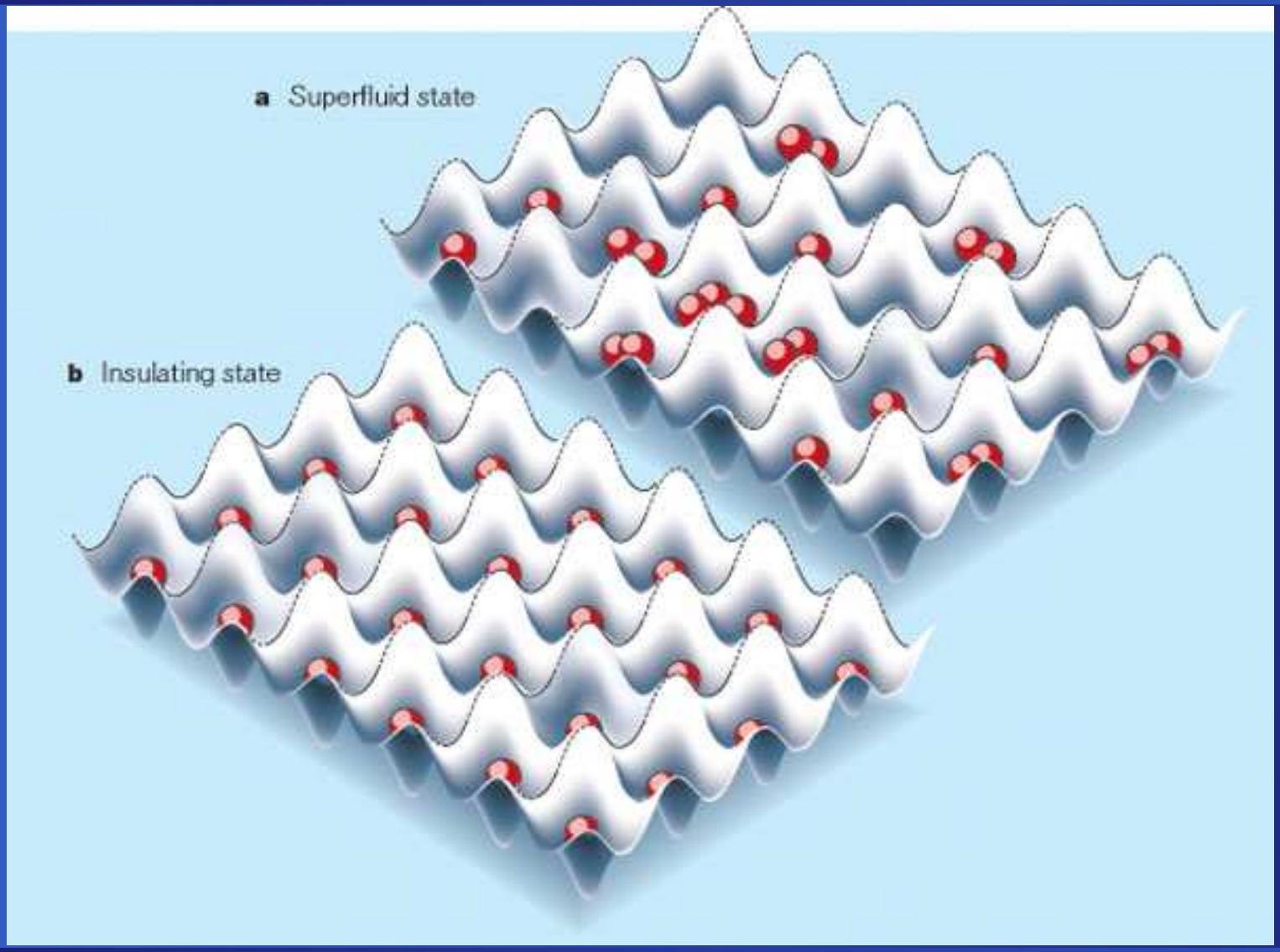

2 - Theoretical description

Bose-Hubbard Hamiltonian:

$$\hat{H}_{\mathrm{BH}} = -t \sum_{\langle i,j \rangle} \hat{a}_i^\dagger \hat{a}_j + \sum_i \left[\frac{U}{2} \hat{n}_i (\hat{n}_i - 1) - \mu \hat{n}_i \right], \qquad \hat{n}_i = \hat{a}_i^\dagger \hat{a}_i$$

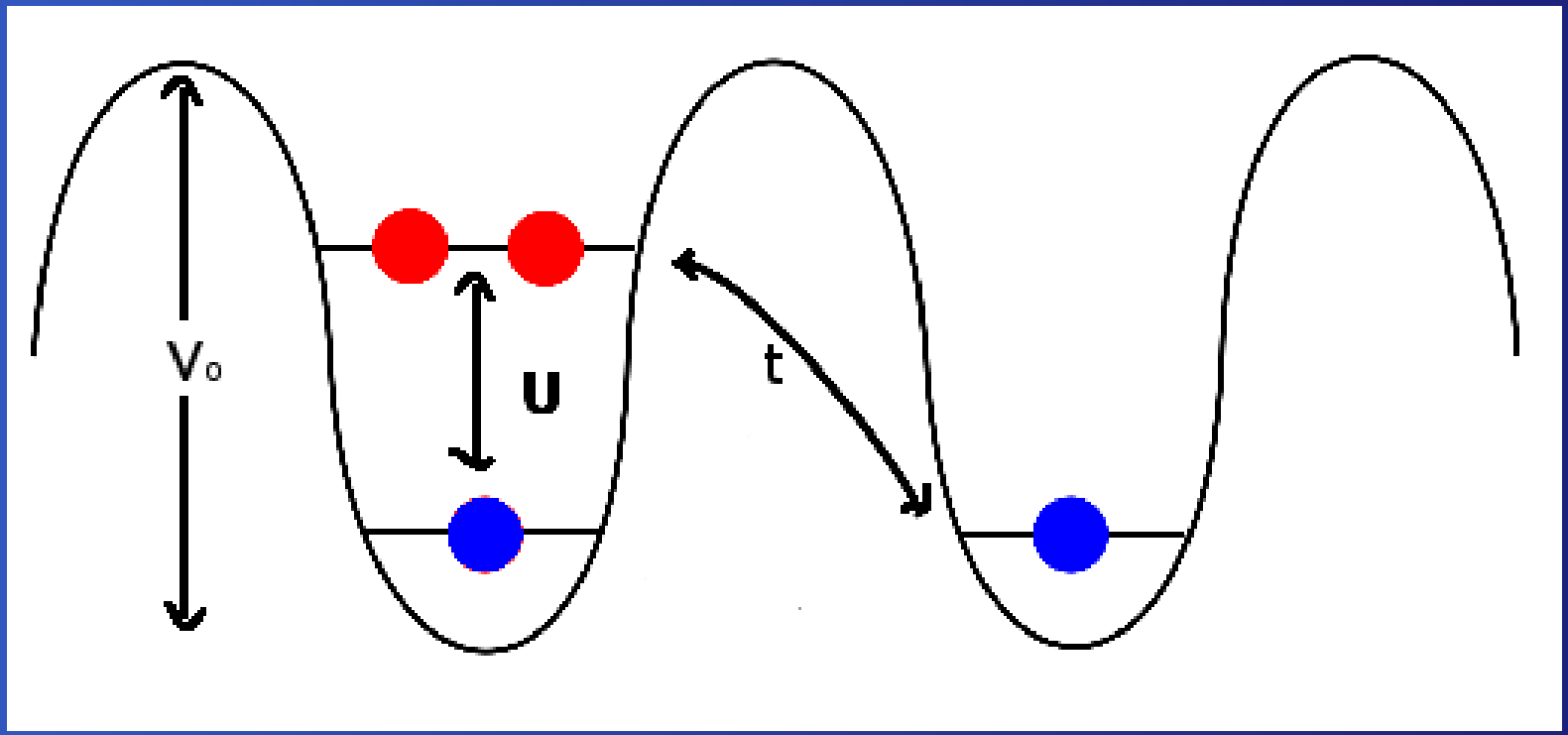

3 - Mean-field theory

Bose-Hubbard Hamiltonian:

$$\hat{H}_{\mathrm{BH}} = -t \sum_{\langle i,j \rangle} \hat{a}_i^\dagger \hat{a}_j + \sum_i \left[\frac{U}{2} \hat{n}_i (\hat{n}_i - 1) - \mu \hat{n}_i \right], \qquad \hat{n}_i = \hat{a}_i^\dagger \hat{a}_i$$

Ansatz: $\sum_{\langle i,j \rangle} \hat{a}_i^\dagger \hat{a}_j \to 2d \sum_i (\psi^* \hat{a}_i + \psi \hat{a}_i^\dagger - |\psi|^2)$

Partition function: $Z = \mathrm{Tr} \left[e^{-\beta \hat{H}_{\mathrm{MF}}(\psi^*, \psi)} \right] = e^{-\beta F_{\mathrm{MF}}(\psi^*, \psi)}$

Self-consistency relations:

$$\begin{cases} \frac{\partial F_{\mathrm{MF}}}{\partial \psi} = 0 \\ \frac{\partial F_{\mathrm{MF}}}{\partial \psi^*} = 0 \end{cases} \Longrightarrow \begin{cases} \langle \hat{a}_i^\dagger \rangle = \psi^* \\ \langle \hat{a}_i \rangle = \psi \end{cases}$$

Landau expansion: $F_{\mathrm{MF}}(\psi^*, \psi) = a_0 + a_2 |\psi|^2 + a_4 |\psi|^4 + \cdots$

If $a_4 > 0$, then $a_2 = 0$ defines the SF-MI phase boundary.

4 - State of the art

Mean-field result:

$$t_c = U/\left[2d\left(\frac{n+1}{n-b}+\frac{n}{1-n+b}\right)\right] \quad , \qquad b=\frac{\mu}{U}$$

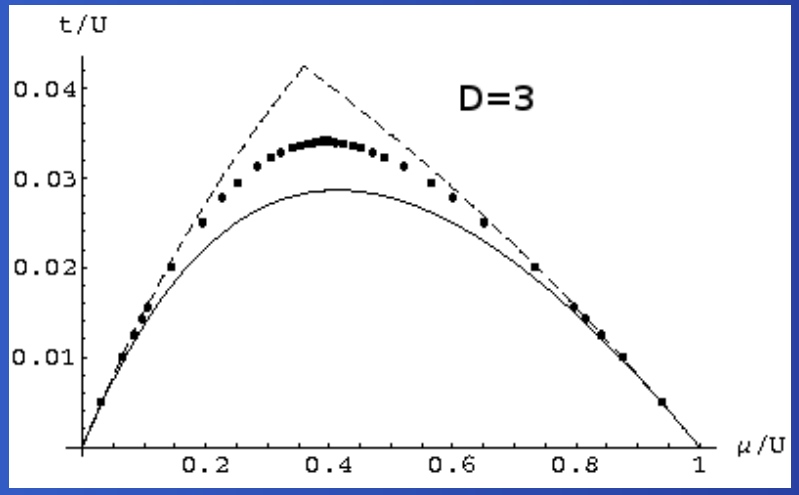

Dashed: 3rd order strong-coupling

Phys. Rev. B, 53:2691, 1996

Line: Mean-field result

Phys. Rev. B, 40:546, 1989

Dots: Monte-Carlo data

Phys. Rev. A, 75:013619, 2007

5 - Effective potential method

Bose-Hubbard Hamiltonian with current:

$$\hat{H}_{\mathrm{BH}}(J^*, J) = \hat{H}_{\mathrm{BH}} + \sum_i \left(J^* \hat{a}_i + J \hat{a}_i^\dagger \right)$$

Partition function: $Z = \mathrm{Tr}\left[e^{-\beta \hat{H}_{\mathrm{BF}}(J^*, J)} \right] = e^{-\beta F_{\mathrm{BH}}(J^*, J)}$

$$\psi = \langle \hat{a}_i \rangle = \frac{1}{N_{\mathrm{s}}} \frac{\partial F(J^*, J)}{\partial J^*} \quad ; \quad \psi^* = \langle \hat{a}_i^\dagger \rangle = \frac{1}{N_{\mathrm{s}}} \frac{\partial F(J^*, J)}{\partial J}$$

Legendre transformation: $\Gamma(\psi^*, \psi) = \psi^* J + \psi J^* - F/N_{\mathrm{s}}$

$$\frac{\partial \Gamma}{\partial \psi^*} = J \quad ; \quad \frac{\partial \Gamma}{\partial \psi} = J^*$$

Physical limit of vanishing current:

$$\frac{\partial \Gamma}{\partial \psi^*} = 0 \quad ; \quad \frac{\partial \Gamma}{\partial \psi} = 0$$

5.1 - Details

$$F(J^*, J) = F_0(t) + \sum_{n=1}^{\infty} c_{2n}(t)|J|^{2n}$$

$$\Gamma(\psi^*, \psi) = -F_0(t) + \frac{1}{c_2(t)}|\psi|^2 - \frac{c_4(t)}{c_2(t)^4}|\psi|^4 + \cdots$$

with: $c_p(t) = \sum_{n=0}^{\infty}(-t)^n \alpha_p^{(n)}$

Phase boundary:

$$\frac{1}{c_2(t_c)} = \frac{1}{\alpha_2^{(0)}}\left\{1 + \frac{\alpha_2^{(1)}}{\alpha_2^{(0)}}t_c + \left[\left(\frac{\alpha_2^{(1)}}{\alpha_2^{(0)}}\right)^2 - \frac{\alpha_2^{(2)}}{\alpha_2^{(0)}}\right]t_c^2 + \cdots\right\} = 0$$

5.2 - Phase boundary

First order: $t_c^{(1)} = -\frac{\alpha_2^{(0)}}{\alpha_2^{(1)}}$

Remark: Identical to mean-field phase boundary.

Second order:

$$t_c^{(2)} = \frac{\overline{\alpha}_1}{2\left(\overline{\alpha}_2 - \overline{\alpha}_1^2\right)} + \frac{1}{2\left(\overline{\alpha}_2 - \overline{\alpha}_1^2\right)}\sqrt{\overline{\alpha}_1^2 - 4\left(\overline{\alpha}_1^2 - \overline{\alpha}_2\right)}$$

with: $\overline{\alpha}_1 = \frac{\alpha_2^{(1)}}{\alpha_2^{(0)}}$; $\overline{\alpha}_2 = \frac{\alpha_2^{(2)}}{\alpha_2^{(0)}}$

Note: Choose the smallest critical $t_c^{(2)}$.

5.3 - Explicit results

$$\alpha_2^{(0)} = \frac{b+1}{U(b-n)(b+1-n)}$$

$$\alpha_2^{(1)} = \frac{2d(b+1)^2}{U^2(b-n)^2(b+1-n)^2}$$

$$\begin{aligned}\alpha_2^{(2)} \quad = \quad & 2\left\{2d(b+1)^3(b-2-n)(b+3-n) + n(b-n)(b+1-n)\right. \\ & \left.\times(1+n)(4+3b+2n)\left[-3-2n+2(b^2+b-2bn+n^2)\right]\right\} \\ & / \left[U^3(b-n-2)(b-n)^3(b+1-n)^3(b+3-n)\right]\end{aligned}$$

Here n is the number of particles at each site and $b = \mu/U$.

6 - Green's function method

- Green's function contains many important information about the system:
  - Quantum phase diagram
  - Time-of-flight pictures
  - Excitation spectra
  - Thermodynamic properties

Imaginary-time Green's function:

$$G_1(\tau', j'|\tau, j) = \frac{1}{Z}\mathrm{Tr}\left\{e^{-\beta\hat{H}_{\mathrm{BH}}}\hat{T}\left[\hat{a}_{j,\mathrm{H}}(\tau)\hat{a}^{\dagger}_{j',\mathrm{H}}(\tau')\right]\right\}$$

with $\hat{a}_{j,\mathrm{H}}(\tau) = e^{\hat{H}\tau/\hbar}\hat{a}_j e^{-\hat{H}\tau/\hbar}$

and $Z = \mathrm{Tr}\left[e^{-\beta\hat{H}_{\mathrm{BF}}}\right] = e^{-\beta F_{\mathrm{BH}}}$.

6.1 - Decomposition

$$\hat{H}_{\mathrm{BH}} = \underbrace{-\sum_{i,j} t_{i,j}\hat{a}_i^\dagger \hat{a}_j}_{\text{perturbation}} + \underbrace{\sum_i \left[\frac{U}{2}\hat{n}_i(\hat{n}_i - 1) - \mu\hat{n}_i\right]}_{\hat{H}^{(0)}}, \qquad \hat{n}_i = \hat{a}_i^\dagger \hat{a}_i$$

Expansion in hopping matrix element:

$$G_1^{(n)}(\tau', i'|\tau, i) = \frac{Z^{(0)}}{Z}\frac{1}{n!}\sum_{i_1,j_1,\ldots,i_n,j_n} t_{i_1 j_1}\ldots t_{i_n j_n}\int_0^\beta d\tau_1 \ldots \int_0^\beta d\tau_n$$
$$\times G_{n+1}^{(0)}(\tau_1, j_1; \ldots; \tau_n, j_n; \tau', i'|\tau_1, i_1; \ldots; \tau_n, i_n, \tau, i)$$

Decomposition into *local* cumulants:

$$G_2^{(0)}(\tau_1', i_1'; \tau_2', i_2'|\tau_1, i_1; \tau_2, i_2) = \delta_{i_1,i_2}\delta_{i_1',i_2'}\delta_{i_1,i_1'} C_2^{(0)}(\tau_1', \tau_2'|\tau_1, \tau_2)$$
$$+\delta_{i_1,i_1'}\delta_{i_2,i_2'} C_1^{(0)}(\tau_1'|\tau_1) C_1^{(0)}(\tau_2'|\tau_2) + \delta_{i_1,i_2'}\delta_{i_2,i_1'} C_1^{(0)}(\tau_2'|\tau_1) C_1^{(0)}(\tau_1'|\tau_2)$$

6.2 - Diagrammatic representation

$= C_1^{(0)}(\tau'|\tau)\,,$

$= C_2^{(0)}(\tau_1', \tau_2'|\tau_1, \tau_2)\,,$

$= t_{ij}$

In Matsubara space with $E_n = \frac{U}{2}n(n-1) - \mu n$:

$$C_1^{(0)}(\omega_m) = \frac{1}{\mathcal{Z}^{(0)}} \sum_{n=0}^{\infty} \left[\frac{(n+1)}{E_{n+1} - E_n - i\omega_m} - \frac{n}{E_n - E_{n-1} - i\omega_m} \right] e^{-\beta E_n}$$

First two orders of perturbation series:

$G_1^{(1)}(\omega_m; i, j) =$

$= t\delta_{d(i,j),1} C_1^{(0)}(\omega_m)^2$

$G_1^{(2)}(\omega_m; i, j) =$

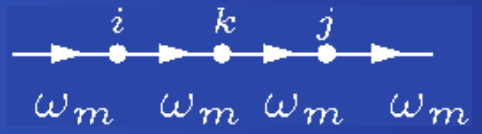

$+$

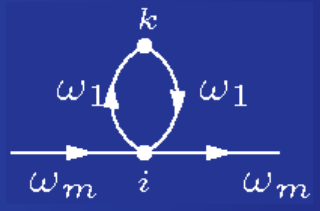

$= t^2(\delta_{d(i,j),2} + 2\delta_{d(i,j),\sqrt{2}} + 2d\delta_{i,j}) C_1^{(0)}(\omega_m)^3$

$+t^2 2d\delta_{i,j} \sum_{\omega_1} C_1^{(0)}(\omega_m) C_2^{(0)}(\omega_m, \omega_1|\omega_m, \omega_1)$

6.3 - Resumation

First-order:

$$\tilde{G}_1^{(1)}(\omega_m; i, j) =$$ 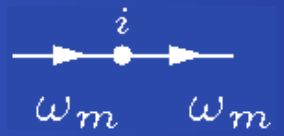

$+$ 

$+$ 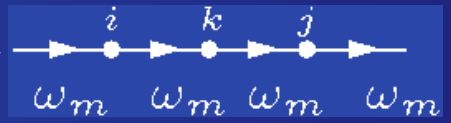

$+\ldots$

Easily summed in Fourier space:

$$\tilde{G}_1^{(1)}(\omega_m, \mathbf{k}) = \frac{C_1^{(0)}(\omega_m)}{1 - t(\mathbf{k})\, C_1^{(0)}(\omega_m)} \quad , \qquad t(\mathbf{k}) = 2t \sum_{l=1}^{d} \cos(k_l a)$$

- Phase boundary given by divergency of $G_1(\omega_m = 0; \mathbf{k} = \mathbf{0})$.
- First-order result reproduces mean-field result
- Improved by taking one-loop diagram into account. Reproduces in zero-temperature limit result of effective potential approach.

7 - Results

Phase diagram for zero temperature:

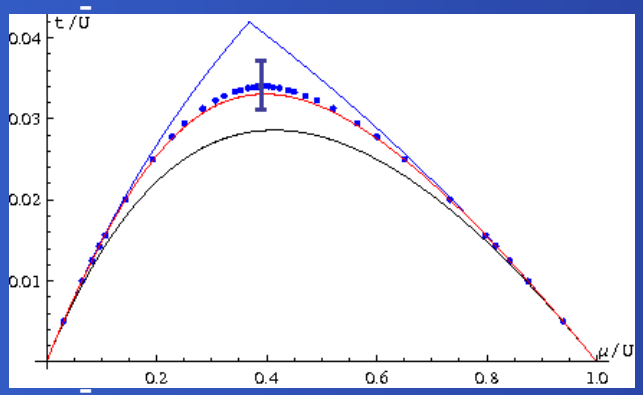

Error bar: Extrapolated strong-coupling series.

Black line: Mean-field.

Blue line: 3rd strong-coupling order.

Red line: Effective potential:
Santos and Pelster, `arXiv:0806.2812`

Blue dots: Monte-Carlo data.

Phase diagram for finite temperature:

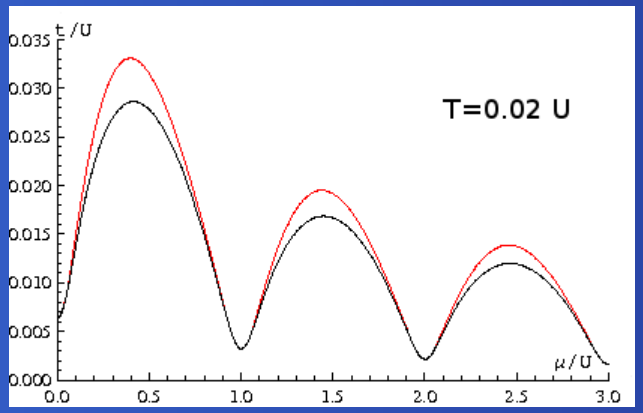

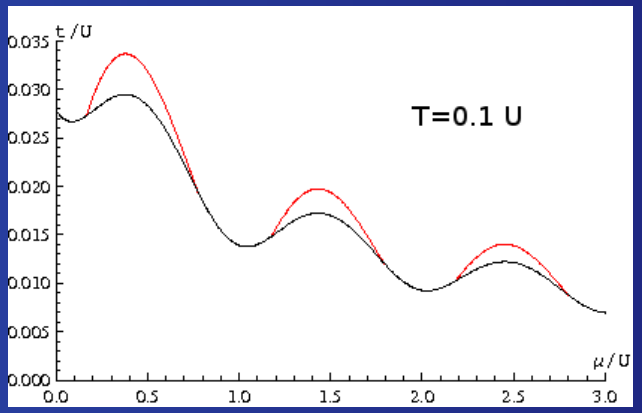

Black: First order (Mean field). Red: Second order (One-loop corrected)

7.1 - More Results

Excitation spectrum:

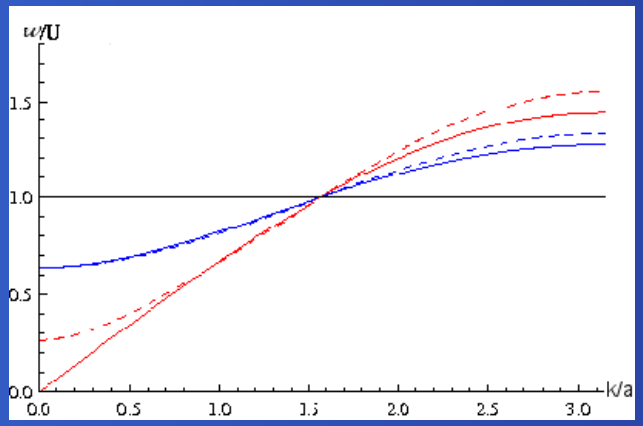

Solid black: $t = 0$.

Solid blue: $t = 0.017\,U$ (first order).

Dotted blue: $t = 0.017\,U$ (second order).

Solid red: $t = 0.029\,U$ (first order).

Dotted red: $t = 0.029\,U$ (second order).

- Excitation spectrum given by poles of real-time Green's function
- Spectrum gapped in Mott phase, becomes gapless at phase boundary
- Only quantitative effects from finite temperature

7.2 - More Results

Time-of-flight pictures:

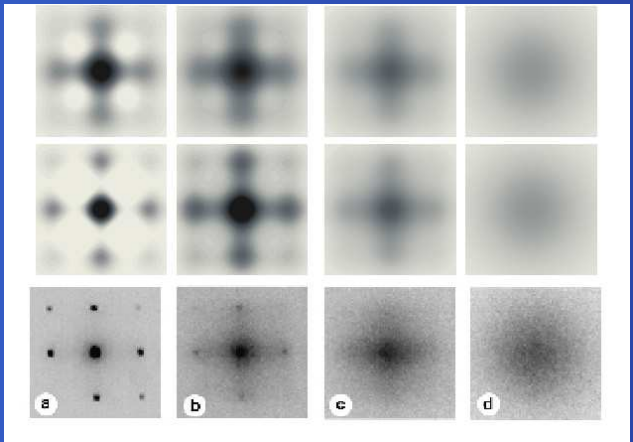

Top to bottom: First-order perturbation theory, Second-order perturbation theory, experiment.

Left to right: $V_0 = 8, 14, 18, 30 E_R$.

Time-of-flight pictures represent momentum distribution:

Hoffmann and Pelster, `arXiv:0809.0771`

Visibility:

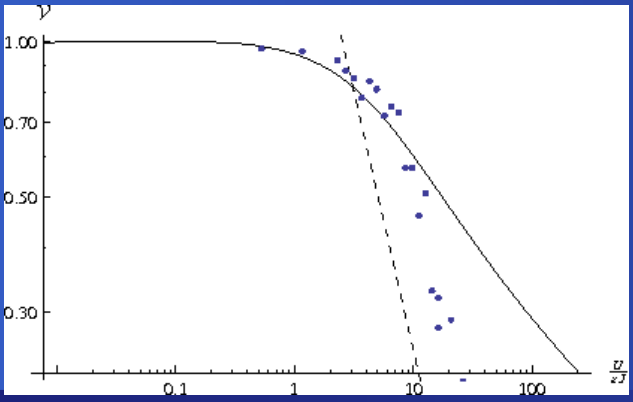

Measure for interference patterns in TOF pictures

$$\nu = \frac{n_{\max} - n_{\min}}{n_{\max} + n_{\min}}$$

Solid: First-order (Wannier functions)

Dashed: First-order (harmonic approximation)

Dots: Experimental data (Bloch's group)

8 - Conclusions

- Monte-Carlo data are believed to be very precise
- Effective potential method gives a difference of 3% from the Monte-Carlo data at the lobe tip.
- Green's function approach allows the calculation of visibility and excitation spectrum. They are candidates for thermometer as they are measurable quantities.
- Effective action method:
  Bradlyn, Santos, and Pelster, arXiv:0809.0706
- Dynamic quantum phase transition – Collapse and Revival